Supporting Information

Trimetallic MOF-Derived CoFeNi/Z-P NC Nanocomposites as Efficient Catalysts for Oxygen Evolution Reaction

Xudun Shen,[a] Liping Huang,[a] Shuaishuai Li,[a] Longnian Tang,[a] Qiumei Lei,[a] Bowang Zhao,[a] Huilian Hao,[a] Wenyao Li*,[a,c], Min Zeng*,[b] and Guanjie He*,[c]

[a] *School of Materials Science and Engineering, Shanghai University of Engineering Science, Shanghai 201620, China.*

[b] *Department of Micro/Nano Electronics, School of Electronic Information and Electrical Engineering, Shanghai Jiao Tong University, 800 Dong Chuan Road, Shanghai, 200240, PR China.*

[c] *Electrochemical Innovation Lab, Department of Chemical Engineering, University College London, London, WC1E 7JE, UK.*

**Corresponding author,*

E-mails: liwenyao314@gmail.com; minzeng@sjtu.edu.cn; g.he@ucl.ac.uk

Structural and electronic property characterization

All scanning electron microscope (SEM) images in this article were taken by Zeiss Gemini300, all transmission electron microscope (TEM) images were taken by FEI TF20, X-ray diffraction (XRD) was taken by SmartLab 9KW, X-ray photoelectron spectroscopy (XPS) was taken by Thermo Scientific K- Alpha, the model of the specific surface area analyzer is JW-BK 200.

Electrochemical measurements

Typically, a mixed solvent made up of 250 μL of ethanol (GCS, 99.5%), 20 μL of a 5 weight percent Nafion solution, and 1 mg of Ketjen Black were used to scatter the catalyst. To get a uniform ink, sonicate the mixture in freezing water for 45 minutes. Then, using the drop-casting method, 10 μL of the ink were applied to a polished glassy carbon electrode (GCE) with a diameter of 5 mm, and left to air dry naturally at room temperature. All electrochemical experiments were performed using a conventional three-electrode cell and the AutoLab 302N electrochemical workstation. In this three-electrode system, the working electrode is a modified GCE electrode, the counter electrode is a graphite rod and the reference electrode is a saturated Ag/AgCl electrode.

Utilizing a scan rate of 5 mV s^{-1}, we employed linear sweep voltammetry (LSV) to analyze the polarization curves for OER activity. All figures were calibrated to a reversible hydrogen electrode (RHE) and corrected for IR correction using the formula $E_{RHE} = E_{Ag/AgCl} + 0.0592\ pH + 0.197$. Using the equation: $\eta(V) = E_{RHE} - 1.23$ V, the overpotential (η) for the hydrogen evolution process (HER) was derived. Electrochemical impedance spectroscopy (EIS) was carried out by applying an AC voltage with a 10 mV amplitude over a frequency range of 1 to 100,000 Hz. Electrical double-layer specific capacitance (C_{dl}) of the materials was determined by cyclic voltammetry (CV) utilizing non-Faradaic overpotentials and sweep rates ranging from 20 to 100 mV s^{-1}.

Figures:

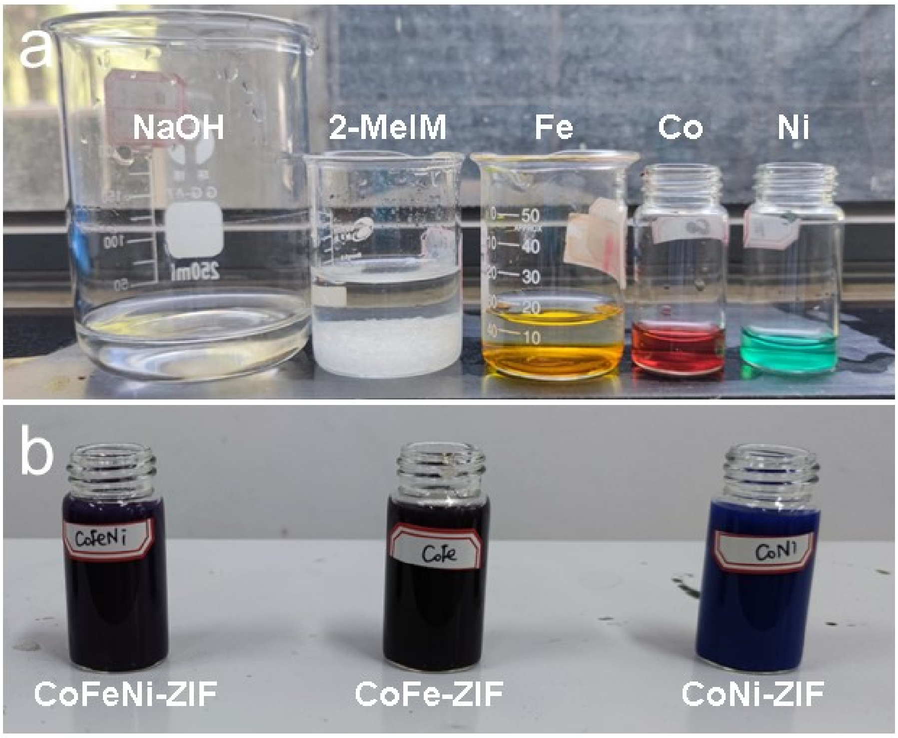

Fig. S1 Optical images of the materials before reaction (a) and after the reaction completed (b)

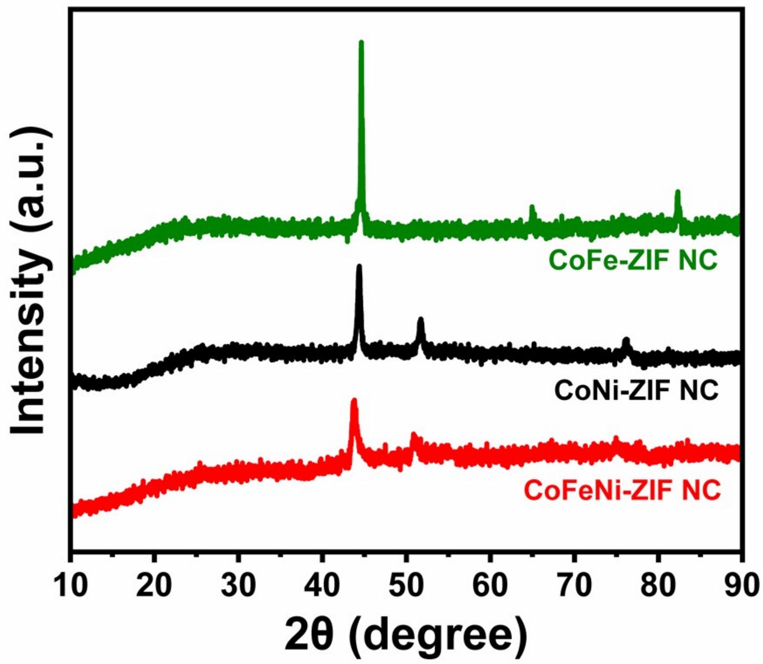

Fig. S2 The XRD patterns of CoFe-ZIF NC, CoNi-ZIF NC and CoFeNi-ZIF NC

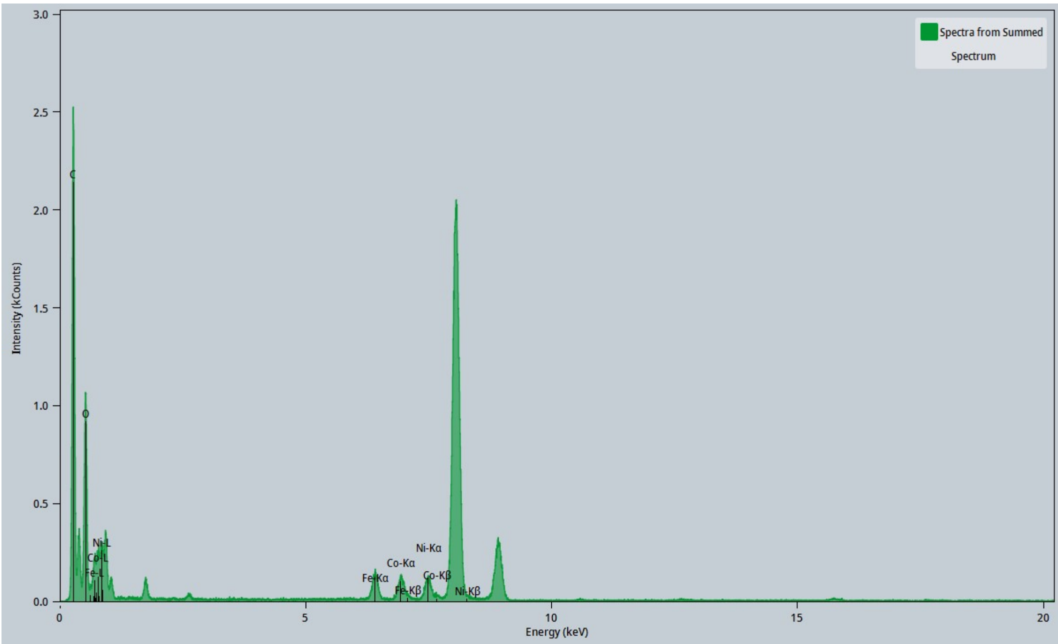

Fig. S3 The EDS composition of CoFeNi-ZIF

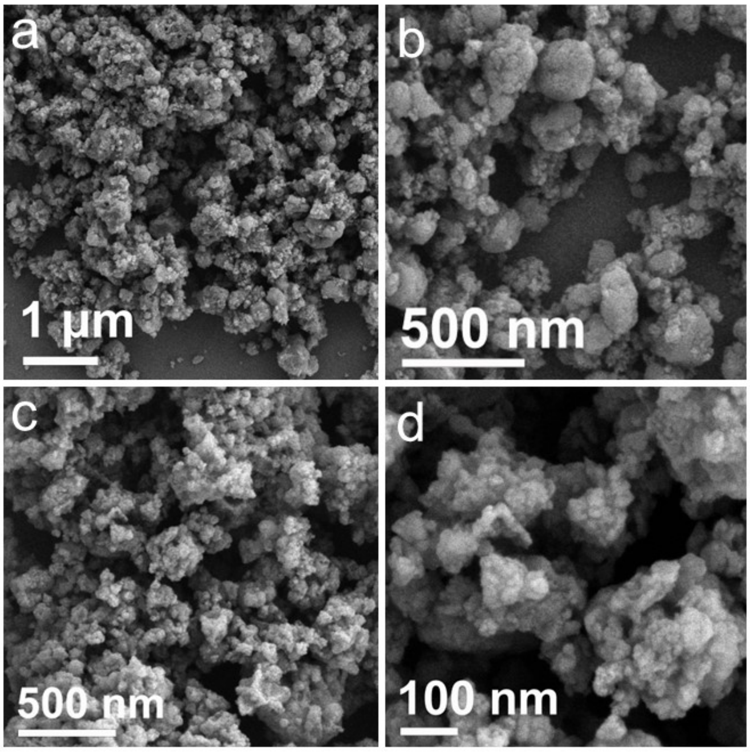

Fig. S4 (a-b) SEM images of CoFeNi-ZIF. (c-d) SEM images of CoFeNi-Z.

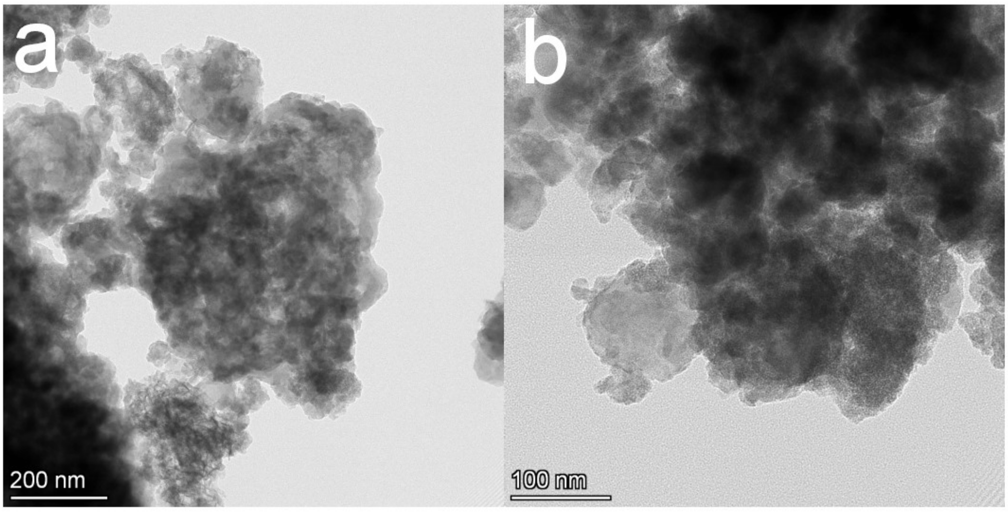

Fig. S5 The TEM images of CoFeNi-Z at 200 nm and 100 nm

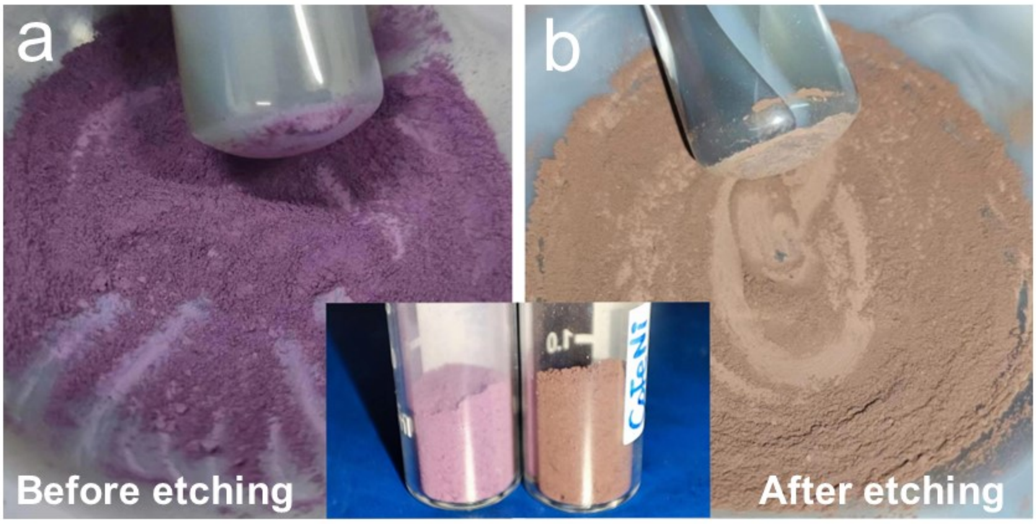

Fig. S6 Optical images of solid samples of CoFeNi-ZIF (a) and CoFeNi-Z (b)

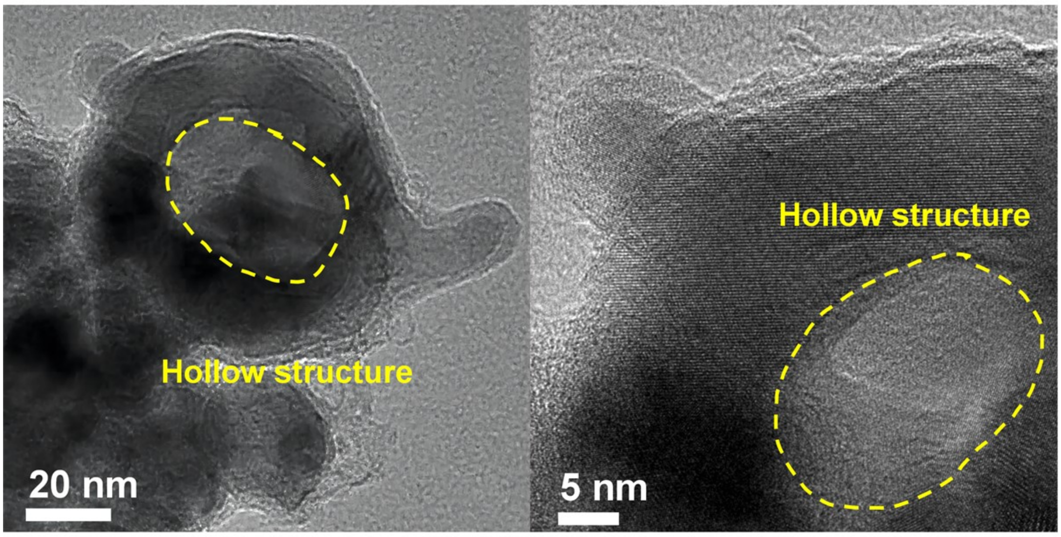

Fig. S7 HRTEM images of CoFeNi/Z-P NC

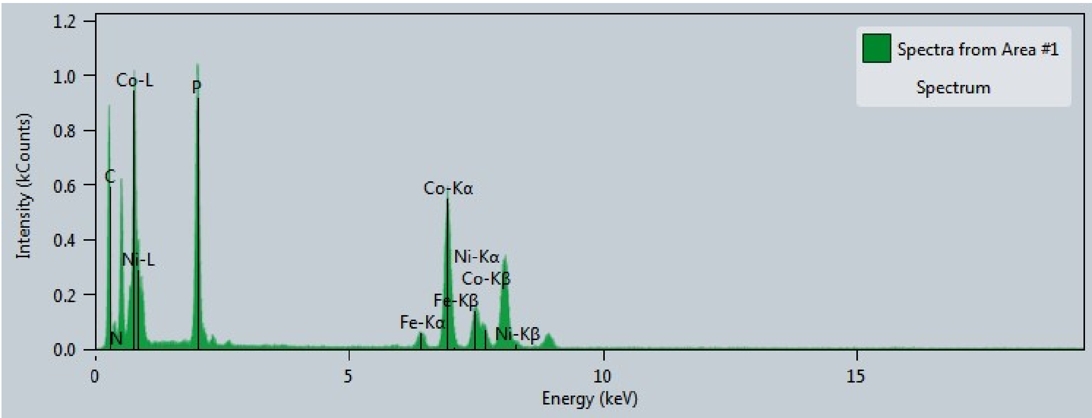

Fig. S8 The EDS composition of CoFeNi/Z-P NC

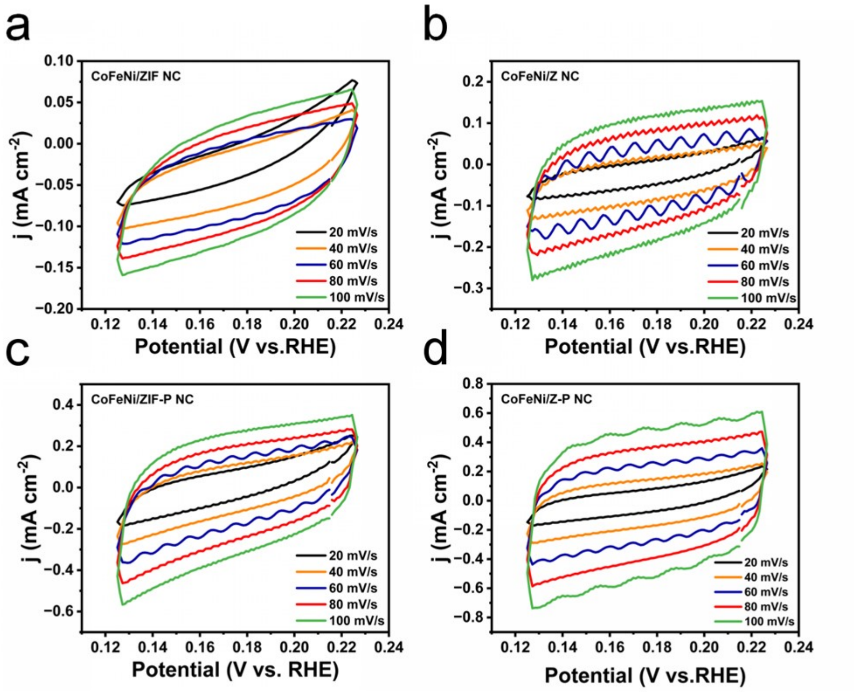

Fig. S9 Cyclic voltammograms of CoFeNi/ZIF NC, CoFeNi/Z NC CoFeNi/ZIF-P NC and CoFeNi/Z P NC within the range of 0.13 to 0.23 V vs RHE with scan rate from 20 to 100 mV s^{-1} in 1 M KOH.

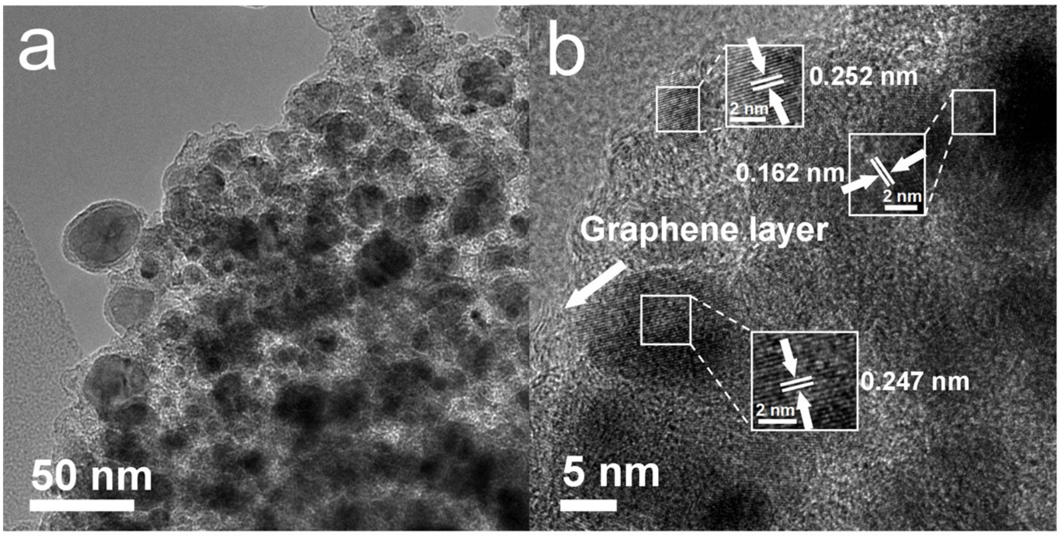

Fig. S10 TEM image and HRTEM image (a and b) of CoFeNi/Z-P NC after stability test

Table S1. Chemical compositions of CoFeNi/Z-P NC by XPS measurement

Sample	C (atom %)	N (atom %)	Co (atom %)	Fe (atom %)	Ni (atom %)	P (atom %)
CoFeNi/Z-P NC	89.88	2.12	1.77	1.63	0.91	3.68

Table S2. Comparison of the OER electrocatalytic performance for different catalysts

Catalyst	**Overpotential (10 mA cm^{-2})**	**Tafel slope (mV dec^{-1})**	**Ref.**
CoFeNi/Z-P NC	244	66.2	**This work**
Fe-Co-N-PC-900	430	93	1
(Co, Ni)Se_2@NiFe LDH	277	114	2
Fe-NiCo-S	247	111	3
NiCoP/NC PHCs	297	51	4
Fe_1Co_1-P/C	360	58.4	5
ZIF-FeCo-F-300	250	51.2	6
Fe_1Co_3–NC-1100	349	99.93	7
CoFeP@C	336	82.5	8
$A_{2.7}$B-MoF-$FeCo_{1.6}$	288	39	9
Co_3O_4/Co-Fe oxide DSNBs	297	61	10

Table S3. Comparison of RuO_2 parameterappearing in the literature

Catalysts	**Electrolyte**	**Overpotential at 10 mA cm^{-2} (vs. RHE)**	**Tafel slope**	**Ref.**
RuO_2	1 M KOH	344 mV	97.4 mV dec^{-1}	**This Work**
RuO_2	1 M KOH	328 mV	130 mV dec^{-1}	3
RuO_2	1 M KOH	378 mV	65.5 mV dec^{-1}	12
RuO_2	1 M KOH	287 mV	108.6 mV dec^{-1}	13
RuO_2	1 M KOH	315 mV	135.7 mV dec^{-1}	14
RuO_2	1 M KOH	327 mV	356.44 mV dec^{-1}	15
RuO_2	1 M KOH	-	141 mV dec^{-1}	8
RuO_2	1 M KOH	332 mV	133.8 mV dec^{-1}	17
RuO_2	1 M KOH	264 mV	192 mV dec^{-1}	18
RuO_2	1 M KOH	298 mV	124 mV dec^{-1}	19
RuO_2	0.1MKOH	380 mV	95 mV dec^{-1}	20

Reference

1. Y. Li, W. Zhou, L. Zheng, J. Liu, R. Tang, K. Shi and Y. Zhang, J. Alloys Compd., 2021, 886, 161227.
2. J. G. Li, H. Sun, L. Lv, Z. Li, X. Ao, C. Xu, Y. Li and C. Wang, ACS Appl. Mater. Interfaces, 2019, 11, 8106-8114.
3. R. Liu, S. Xu, X. Shao, Y. Wen, X. Shi, L. Huang, M. Hong, J. Hu and Z. Yang, ACS Appl Mater Interfaces, 2021, 13, 47717-47727.
4. X. Zhang, L. Huang, Q. Wang and S. Dong, J. Mater. Chem. A, 2017, 5, 18839-18844.
5. W. Hong, M. Kitta and Q. Xu, Small Methods, 2018, 2, 1800214.
6. X. Gu, Y. G. Ji, J. Tian, X. Wu and L. Feng, Chem. Eng. J., 2022, 427, 131576.
7. Y. He, X. Yang, Y. Li, L. Liu, S. Guo, C. Shu, F. Liu, Y. Liu, Q. Tan and G. Wu, ACS Catal., 2022, 12, 1216-1227.
8. L. Gao, S. Chang and Z. Zhang, ACS Appl. Mater. Interfaces, 2021, 13, 22282-22291.
9. Z. Xue, Y. Li, Y. Zhang, W. Geng, B. Jia, J. Tang, S. Bao, H.-P. Wang, Y. Fan, Z. Wei, Z. Zhang, Z. Ke, G. Li and C. Su, Adv. Energy Mater., 2018, 8, 1801564.
10. X. Wang, L. Yu, B. Y. Guan, S. Song and X. W. Lou, Adv. Mater., 2018, 29, 1801211.
11. Z. Wang, S. Li, G. Zhang, X. Yu, Y. Shi, Y. Zhang and X. Xiao, J. Alloys Compd., 2023, 933, 167787.
12. C. Zhang, W. Xu, S. Li, X. Wang, Z. Guan, M. Zhang, J. Wu, X. Ma, M. Wu and Y. Qi, Chem. Eng. J., 2023, 454, 140291.
13. L. Zhang, Y. Bao, Y. Chen, Q. Zhang, N. Zhang, J. Zhang and Z. Liu, J. Alloys Compd., 2023, 937, 168373.
14. Y. Li, M. Yuan, H. Yang, K. Shi, Z. Sun, H. Li, C. Nan and G. Sun, Appl. Catal. B- Environ., 2023, 323, 122167.
15. F. Li, J. Li, L. Zhou and S. Dai, Sustainable Energy Fuels, 2021, 5, 1095–1102.
16. G. Zhang, Y. Li, X. Xiao, Y. Shan, Y. Bai, H. Xue, H. Peng, Z. Tian and Q. Xu,

Nano Lett., 2021, 21, 3016−3025.

17. Z. Guo, Y. Ma, Y. Zhao, Y. Song, S. Tang, Q. Wang and W. Li, J. Power Sources, 2022, 542, 231723.

18. Q, Shi, Q. Liu, Y. Ma, Z. Fang, Z. Liang, G. Shao, B. Tang, W. Yang, L. Qin and X. Fang. Adv. Energy Mater., 2020, 10, 1903854.